Journal of Materials Chemistry

Cite this: J. Mater. Chem., 2012, 22, 14856

www.rsc.org/materials

COMMUNICATION

All carbon nanotube fiber electrode-based dye-sensitized photovoltaic wire†

Fangjing Cai, Tao Chen and Huisheng Peng*

Received 11th April 2012, Accepted 26th June 2012
DOI: 10.1039/c2jm32256k

Carbon nanotubes (CNTs) have been recently spun into macroscopic fiber, in which CNTs are highly aligned along the axial direction, providing excellent mechanical and electrical properties for a wide variety of applications. One CNT fiber adsorbed with dye molecules functions as working electrode, while another CNT fiber is used as counter electrode. Two fiber electrodes are twined to produce the desired photovoltaic wire with high promise in many applications. In particular, this photovoltaic wire can be woven into textiles or integrated into various flexible equipment which remains challenging to the conventional planar solar cells.

Introduction

Carbon nanotubes (CNTs) have been widely introduced into organic photovoltaics with improved performance due to their large surface area, excellent electrical and electrocatalytic properties.[1,2] They can be directly incorporated into photoactive layer to enhance separation and transport of electrons and holes.[3–5] Also, They have been assembled into free-standing films to be widely used as counter electrodes in replacement of platinum electrode to catalyze the redox reaction of electrolyte in dye-sensitized solar cells.[6–9] However, the reported CNTs were typically distributed randomly in the photoactive layer or electrode, which greatly limited the photovoltaic performance of the resulting cells.[10–12] Therefore, highly aligned CNTs in formats of films and fibers have recently attracted increasing attentions.[13,14] Aligned CNT materials have well maintained the excellent physical and chemical properties of individual CNTs, such as high mechanical strength, excellent electrical conductivity, and remarkable electrocatalytic activity. Dye-sensitized solar cells with high efficiency have been obtained by using aligned CNT sheets replacing Pt as counter electrode.[13]

On the other hand, dye-sensitized solar cells have been widely explored due to their easy fabrication, high efficiency, and low cost.[15,16] For instance, their energy conversion efficiencies can achieve 12%.[17,18] However, in the conventional dye-sensitized solar cells with planar structure, rigid indium tin oxide (ITO) or fluorine-doped tin oxide (FTO) coated glass was used as the transparent conductive substrate, which has greatly hindered their applications such as self-power generators and portable equipments.[19,20] To this end, photovoltaics in the format of wires are proposed as an effective solution and have started to attract extensive attention in recent years.[21–26] In a photovoltaic wire, metal wires such as copper and steel wires or polymer fibers coated with a conductive layer of ITO are usually used as the fiber-shaped conductive substrate.[21–24] However, the performances of photovoltaic wires are much lower than expected due to the limited flexibility and low stability of electrodes.[27,28] New fiber electrode materials are highly desired to improve the performance of photovoltaic wire.

It should be noted that the CNT fiber had been also used as a working electrode to fabricate planar dye-sensitized solar cells in our previous work.[2] A power conversion efficiency of 2.2% had been achieved. However, the above cell appeared in a conventional planar structure. Of course, it could not be woven into textiles or integrated into the other flexible devices. In addition, noble metal platinum was required for the counter electrode.

Herein, we have developed a novel photovoltaic wire without using any metal electrode. The structure of the photovoltaic wire is schematically shown in Fig. 1a, and the working mechanism is further summarized in Fig. 1b. A CNT fiber absorbed with N719 is used as working electrode, while a CNT fiber with a thin layer of PVDF on the outer surface is used as counter electrode. The above two CNT fiber-based electrodes are twined together to produce the designed photovoltaic wire. These photovoltaic wires can be easily integrated into textiles or other deformable structures through a conventional weaving technique.

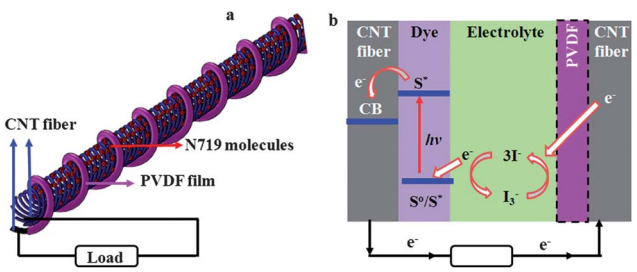

Fig. 1 (a) Schematic illustration of a photovoltaic wire with two twined CNT fibers as working and counter electrodes, respectively. (b) The working principle of the CNT fiber-based sensitized photovoltaic wire, in which CB represents conduction band of carbon nanotube.

State Key Laboratory of Molecular Engineering of Polymers, Department of Macromolecular Science, and Laboratory of Advanced Materials, Fudan University, Shanghai 200438, China. E-mail: penghs@fudan.edu.cn

† Electronic supplementary information (ESI) available. See DOI: 10.1039/c2jm32256k

Experimental section

Preparation of CNT and CNT/PVDF composite fiber

Spinnable CNT arrays were synthesized by a chemical vapor deposition in a quartz tube furnace.[29–31] Fe (1.2 nm)/Al_2O_3 (3 nm) on silicon wafer was used as the catalyst, ethylene was used as carbon source with a flow rate of 90 sccm, a mixture of Ar (400 sccm) and H_2 (30 sccm) was used as the carrier gas, and the reaction was carried out at 750 °C typically for 10 min. CNT fibers were then spun from the arrays through a rotating microprobe with rotary speed of 2000 rad min^{-1} during the spinning process.

The CNT/poly(vinylidene fluoride) (PVDF) fiber was prepared by dipping one end of the as-prepared CNT fiber with lengths of 1–3 cm into PVDF solutions in *N*,*N*-dimethyl formamide (DMF) with concentrations of 2, 10 and 20 mg mL^{-1}, respectively. Note that the other end of the CNT fiber should not be coated with the polymer for the connection with the external circuit.

Fabrication of the photovoltaic wire

The fabrication process of a typical wire cell was summarized as below. An as-prepared CNT fiber was heated to 120 °C, followed by immersion of one end into the solution of 0.3 mM [*cis*-bis(isothiocyanato)bis(2,2′-bipyridyl-4,4′-dicarboxylato) ruthenium(II) bistetrabutylammonium] (also called N719) in a mixture solvent of alcohol and isopropanol (volume ratio of 1 : 1) at room temperature overnight. The resulting CNT/N719 composite fiber was then taken out of the N719 solution, followed by evaporation of solvents in air. The CNT/N719 composite fiber and CNT/PVDF composite fiber were fixed onto a glass slide by adhesive tape and twined together carefully. The other ends of the two fibers were also fixed on a glass slide with indium through ultrasonic welding technique to connect the external circuit. The electrolyte of 0.1 M lithium iodide, 0.05 M iodine, 0.6 M 1,2-dimethyl-3-propylimidazolium iodide, and 0.5 M 4-*tert*-butyl-pyridine in dehydrated acetonitrile was finally dropped onto the assembled device prior to *I*–*V* characterizations.

Characterization

The structures of CNT fiber and its composite fibers were characterized by scanning electron microscopy (SEM, Hitachi S-4800 operated at 1 kV) and transmission electron microscopy (TEM, JEOL JEM-2100F operated at 200 kV). Tensile strength–strain curves were obtained from a Shimadzu Table-Top Universal Testing Instrument. A CNT fiber was mounted on a paper tab with gauge length of 5 mm, and the fiber diameter was measured by SEM. Raman measurements were performed on Renishaw inVia Reflex with excitation wavelength of 514.5 nm and laser power of 20 mW at room temperature. Cyclic voltammograms were obtained from a CHI 660a electrochemical workstation at room temperature, and the experiments were performed through a three-electrode system with a CNT fiber or CNT/PVDF composite fiber (2 cm in length) as working electrode, Pt wire as counter electrode, and Ag/AgCl filled with saturated KCl as reference electrode. An acetonitrile solution containing 0.1 M $LiClO_4$, 5 mM LiI, and 0.5 mM I_2 was used as electrolyte. The *I*–*V* curves of the dye-sensitized photovoltaic wires were measured with a Keithley 2400 Source Meter under illumination (100 mW cm^{-2}) of simulated AM 1.5 solar light coming from a solar simulator (Oriel-Sol3A 94023A equipped with a 450 W Xe lamp and an AM1.5 filter). The light intensity was calibrated using a reference Si solar cell (Oriel-91150). The effective area used to calculate the current density of the photovoltaic wire was obtained by multiplying the diameter and length of the fiber.

Results and discussion

To fabricate the photovoltaic wire, the CNT fibers were first spun from CNT arrays. The thickness of the used spinnable CNT array was ~170 μm in this work. Fig. S1a and b† show the side view of an array at low and high magnifications by SEM. Obviously, CNTs are perpendicular to the substrate and highly aligned with each other. Fig. S1c and d† are typical TEM images of spinnable CNTs with multi-walled structure and diameter of ~8 nm. Fig. 2a and c show SEM images of an as-prepared CNT fiber with diameter of ~16 μm, in which the CNTs remain highly aligned. Due to the high alignment of building CNTs inside,[2,29–31] CNT fibers maintain properties of individual carbon nanotubes, exhibiting excellent mechanical and electrical properties. Herein, the tensile strength of a CNT fiber is as high as 800 MPa (Fig. S2†), while the electrical conductivity of a CNT fiber can easily achieve ~316 S cm^{-1}. The as-prepared CNT fiber was immersed into the dye solution, followed by evaporation of solvent to produce the CNT/N719 composite fiber. The diameter of

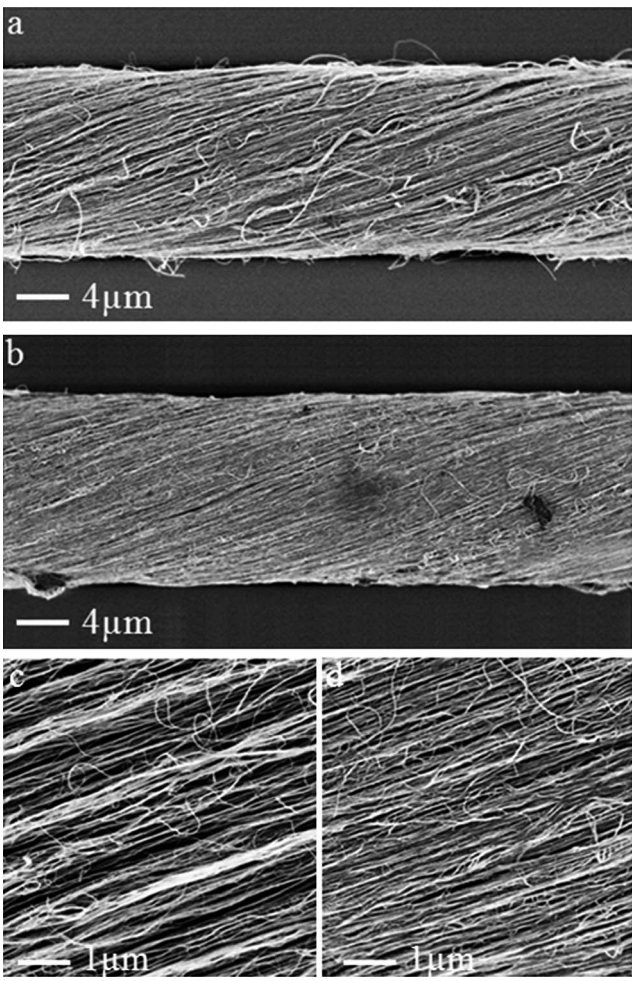

Fig. 2 SEM images of a CNT fiber before (a and c) and after (b and d) formation of the composite with N719.

the composite fiber was decreased for ~2 μm during the evaporation of solvent. Fig. 2b and d show typical SEM images of this composite fiber. The distance among CNTs was decreased, while the CNTs maintained the highly aligned structure. Therefore, the excellent mechanical and electrical properties could be well retained.

N719 molecules can be adsorbed onto the surface of CNTs due to the strong interaction between the pyridine rings of N719 molecules and CNTs, which had been confirmed by Raman spectra (Fig. S3†).[33] After the composite fiber formed, the peaks at 1260 and 1290 cm^{-1} which correspond to C–C ring and C–O stretching modes in N719 shift to higher frequencies of 1268 and 1312 cm^{-1}, respectively. In addition, for the bipyridine vibration, the peak at 1469 cm^{-1} shifts to a higher frequency of 1478 cm^{-1}, while the peaks at 1536 and 1607 cm^{-1} shift to lower frequencies of 1540 and 1603 cm^{-1} respectively. The Raman shifts are attributed to the coupling effect between N719 molecule and CNT, which also indicates the absorption of N719 on CNT fiber.[2,32] Note that for a bare CNT fiber, the G-band is much stronger than that of the D-band, which indicates that the building CNTs were very clean with less amorphous carbon or other impurities.

A short circuit will be caused if a CNT/N719 composite fiber as working electrode was directly twined with a bare CNT fiber as counter electrode to fabricate the dye-sensitized photovoltaic wire. To avoid the short circuit, a thin layer of PVDF film with porous structure was coated onto the outer surface of a bare CNT fiber. PVDF was used due to its exceptional properties including high mechanical strength, good thermal stability, and high chemical resistance.[33] In particular, the formation of porous structure in PVDF layer provides channels for effective transport of ions and electrons. It has been already widely used in lithium ion batteries.[34] Here, PVDF was used, which not only can prevented the short circuit but also improved the performance of photovoltaic wire. The CNT fiber could not be completely covered with a layer of PVDF when the concentration of PVDF in DMF was lower than 5 mg mL^{-1} (Fig. 3a and c), as a result of that it could not effectively prevent the short circuit. With the increase of PVDF concentration to 10 mg mL^{-1}, a perfect PVDF film with desired porous structure was obtained (Fig. 3b and d). With further increasing the PVDF concentration to higher than 10 mg mL^{-1}, the resulting fibers became non-uniform in both morphology and diameter because of the serious aggregation of the polymer, which will cause ineffective contact between two electrodes in the photovoltaic wire.

To evaluate the possibility of CNT fiber as a counter electrode in the dye-sensitized photovoltaic wire, cyclic voltammetry (CV) was carried out to study the electrocatalytic capability of CNT fiber towards to the redox reaction of I^-/I_3^- couple.[6–9] Fig. 4a shows CV spectra of a bare CNT fiber and a CNT/PVDF composite fiber with two pairs of redox peaks in both cases. The left and right redox peaks correspond to reactions (1) and (2), respectively.

$$3I^- \leftrightarrow I_3^- + 2e \quad (1)$$

$$2I_3^- \leftrightarrow 3I_2 + 2e \quad (2)$$

Due to the porous structure of the PVDF layer, the CNT/PVDF composite fiber shows almost the same current value for the redox peaks as a bare CNT fiber (Fig. 4a), which indicates a similar electrocatalytic capability towards the redox reaction of I^-/I_3^- couple.

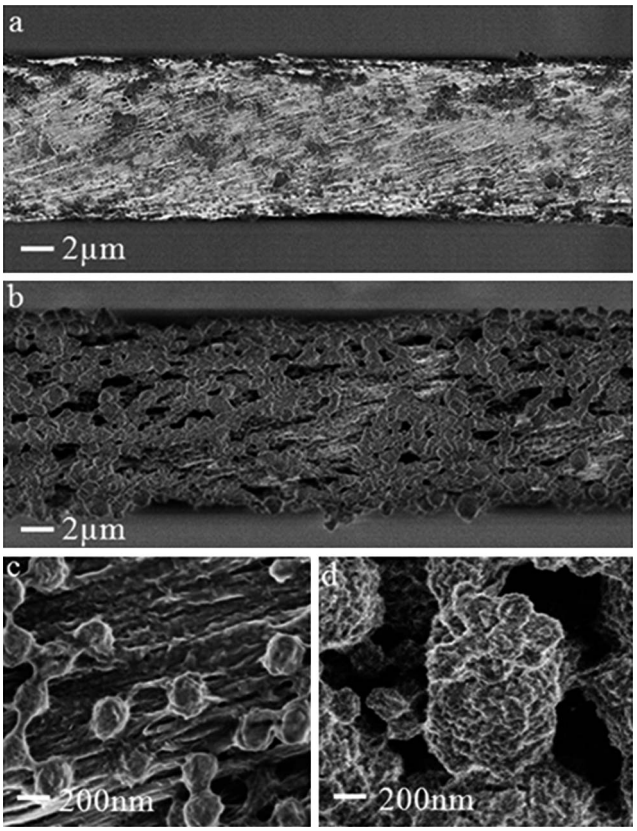

Fig. 3 SEM images of composite fibers with the CNT as the core and PVDF as the sheath. (a and c) A composite fiber prepared by dipping a pure CNT fiber in the PVDF solution with concentration of 2 mg mL^{-1}. (b and d) A composite fiber prepared by dipping a pure CNT fiber in the PVDF solution with concentration of 10 mg mL^{-1}.

This result also shows that the porous PVDF layer can provide effective transport channels for the ions. Fig. 4b further exhibit CV spectra of a CNT/PVDF composite fiber at different scanning rates, from which the relationship between the redox current *versus* square root of scanning rate can be obtained (inserted graph in Fig. 4b). The linear relationship indicates that the redox reaction of I^-/I_3^- redox couples on the CNT/PVDF composite fiber is controlled by an ionic diffusion process.[35]

Fig. 5 shows SEM images of one part of a dye-sensitized photovoltaic wire which was fabricated by using CNT/PVDF composite

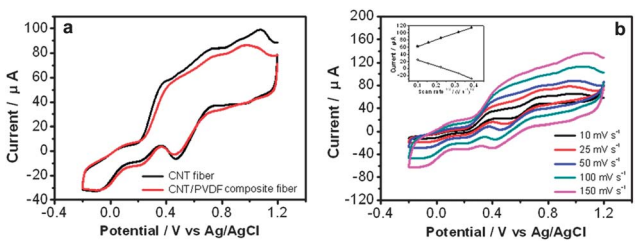

Fig. 4 (a) Typical cyclic voltammetry spectra of a CNT fiber and a CNT/PVDF composite fiber at the scanning rate of 50 mV s^{-1}. (b) Cyclic voltammetry spectra of CNT/PVDF composite fiber at different scanning rate, the inset figure shows the dependence of redox peak current on the square root of the scanning rate.

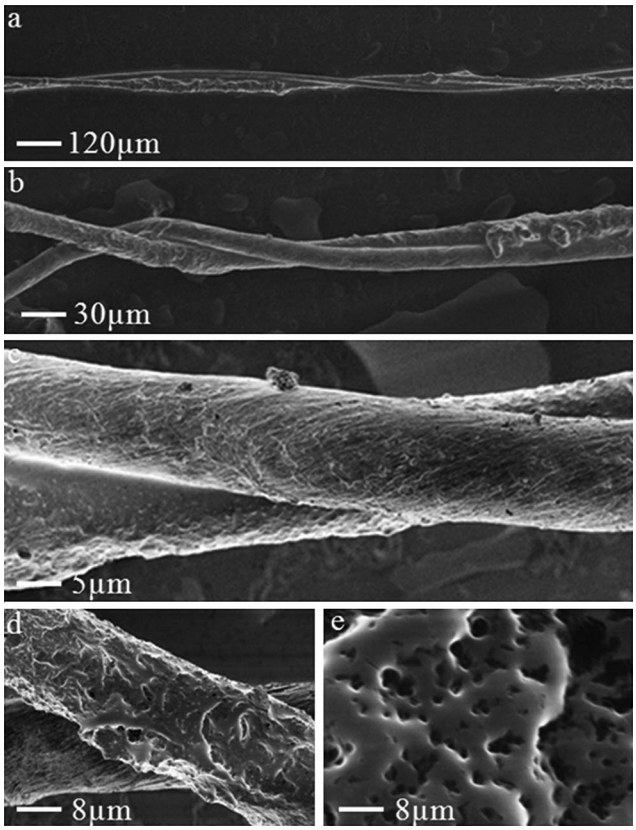

Fig. 5 SEM images of a photovoltaic wire. (a–d) One part under different magnifications. (e) PVDF layer coated on the outer surface of a CNT fiber.

fiber prepared from a PVDF concentration of 10 mg mL^{-1}. The dye-absorbed CNT fiber can be closely twined and contacted with the CNT/PVDF fiber, which is critical for efficient charge transport in the photovoltaic wire. This may be derived from the fact that the highly flexible property of pure CNT fibers had been well maintained in both CNT/N719 and CNT/PVDF composite fibers. In addition, the similar diameters of two composite fibers may also favor an effective contact between them. Fig. 5e further shows a SEM image of PVDF film at high magnification. A porous structure with pore sizes ranging from hundreds of nanometers to a few micrometers was clearly observed, which can provide enough space for electrolyte and pathway for ions.

Typical *J–V* curves of these dye-sensitized photovoltaic wires are shown in Fig. 6a under illumination of simulated AM 1.5 (100 mW cm^{-2}) solar light. For the wire cells derived from the CNT/PVDF fibers which were prepared from different PVDF concentrations, both open-circuit voltage and short-circuit current obviously increase with increasing PVDF concentrations from 2 to 10 mg mL^{-1}, then decrease with further increasing of PVDF concentration to 20 mg mL^{-1}. As shown in Fig. 5, the structure of PVDF layer on the CNT fiber was determined by the PVDF concentration in DMF. A uniform and continuous PVDF layer with porous structure was most effectively achieved at 10 mg mL^{-1}, which produced the photovoltaic wire with the highest efficiency. At this concentration point, the open-circuit voltage, short-circuit current density, and fill factor were typically 0.08 V, 3.4 mA cm^{-2}, and 0.23, respectively. These dye-sensitized photovoltaic wires can be easily organized in series or parallel connection. Fig. 6b shows typical *I–V* curves of two photovoltaic wires and their assembly in series and parallel connections. The short-circuit current of two wire cells in parallel connection approached the sum of short-circuit currents in two individual ones, while the open-circuit voltage of two wire cells in series connection was almost the sum of open-circuit voltages in two individual ones. Currently, the power conversion efficiency of photovoltaic wires is relatively low, which can be partly ascribed to the low absorption of N719 on CNTs and mismatch of energy levels between N719 and CNTs. The dye-sensitized solar cell could be stable for four weeks after sealing.

The power conversion efficiency had been greatly increased if other semiconductive nanomaterials such as titanium dioxide were introduced. Fig. 7a shows a typical *J–V* curve with open-circuit voltage of 0.63 V, short-circuit current density of 7.72 mA cm^{-2}, and fill factor of 0.48, which produces a power conversion efficiency of 2.32% by introduction of titanium dioxide nanoparticles in the photovoltaic wire. In the case of aligned titanium dioxide nanotubes which were perpendicular to the outer surface of the working electrode, the resulting cell showed a typical *J–V* curve with open-circuit voltage of 0.69 V, short-circuit current density of 9.84 mA cm^{-2}, and fill factor of 0.57, which produces a power conversion efficiency of 3.90% (Fig. 7b). The further improvement may be explained by the fact that the produced charges can be more effectively separated along the aligned titanium dioxide nanotubes compared with a lot of interfaces among nanoparticles. More efforts are underway.

To further investigate the advantage of CNT fiber as counter electrode, we had tried to fabricate a photovoltaic wire by using N719-absorbed CNT fiber as working electrode while platinum wire

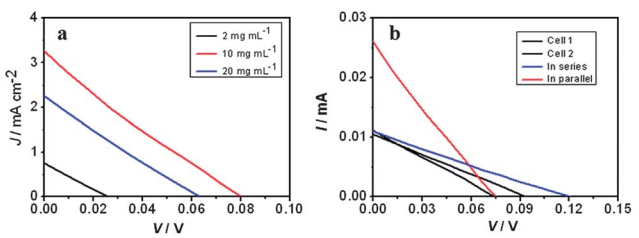

Fig. 6 (a) *J–V* curves of photovoltaic wires by using CNT/PVDF fibers prepared with different PVDF concentrations in *N*,*N*-dimethyl formamide as counter electrodes when the similar CNT/N719 composite fiber was used as working electrode. (b) *I–V* curves of two photovoltaic wires as well as their series and parallel connections.

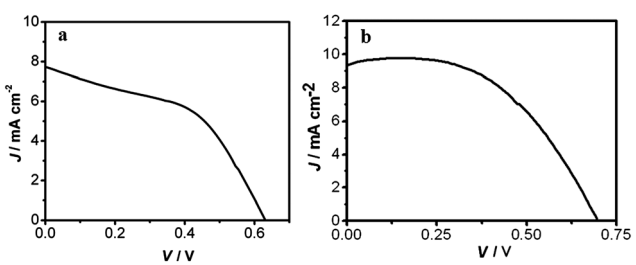

Fig. 7 *J–V* curves of photovoltaic wires on the basis of modified working electrodes. (a) Titanium dioxide nanoparticles on the CNT fiber as the working electrode. (b) Aligned titanium dioxide nanotubes on the titanium wire as the working electrode.

as counter electrode, and a short circuit was produced. Similarly, we had also tried to coat a layer of PVDF on the platinum wire to prevent the short circuit. However, it remained challenging to obtain a uniform and continuous PVDF layer on the platinum wire with smooth surface which was required by the wire device.

Conclusion

In summary, through a low-cost and high-efficiency solution process, we have designed and fabricated a novel dye-sensitized photovoltaic wire, in which CNT/N719 and CNT/PVDF fibers were used as working and counter electrodes in replacement of metal wire electrode, respectively. The power conversion efficiency of this kind of photovoltaic wires could be greatly improved through modification at the working electrode, *e.g.*, incorporation of titanium dioxide nanomaterials.

Acknowledgements

This work was supported by NSFC (20904006, 91027025), MOST (2011CB932503, 2011DFA51330), MOE (NCET-09-0318), and STCSM (1052nm01600, 11520701400).

References

1 L. Hu, D. S. Hecht and G. Grüner, *Chem. Rev.*, 2010, **110**, 5790–5844.
2 T. Chen, S. Wang, Z. Yang, Q. Feng, X. Sun, L. Li, Z. Wang and H. Peng, *Angew. Chem., Int. Ed.*, 2011, **50**, 1815–1819.
3 S. Berson, R. de Bettignies, S. Bailly, S. Guillerez and B. Jousselme, *Adv. Funct. Mater.*, 2007, **17**, 3363–3370.
4 C. Li, Y. Chen, Y. Wang, Z. Iqbal, M. Chhowalla and S. Mitra, *J. Mater. Chem.*, 2007, **17**, 2406–2411.
5 M. W. Rowell, M. A. Topinka, M. D. McGehee, H. J. Prall, G. Dennler, N. S. Sariciftci, L. B. Hu and G. Gruner, *Appl. Phys. Lett.*, 2006, **88**, 233506.
6 S. Zhang, C. Ji, Z. Bian, R. Liu, X. Xia, D. Yun, L. Zhang, C. Huang and A. Cao, *Nano Lett.*, 2011, **11**, 3383–3387.
7 W. J. Lee, E. Ramasamy, D. Y. Lee and J. S. Song, *ACS Appl. Mater. Interfaces*, 2009, **1**, 1145–1149.
8 J. Han, H. Kim, D. Y. Kim, S. M. Jo and S. Jang, *ACS Nano*, 2010, **4**, 3503–3509.
9 B. Pradhan, S. K. Batabyal and A. J. Pal, *Appl. Phys. Lett.*, 2006, **88**, 093106.
10 Y. Kanai and J. C. Grossman, *Nano Lett.*, 2008, **8**, 908–912.
11 H. Peng, *J. Am. Chem. Soc.*, 2008, **130**, 42–43.
12 J. E. Trancik, S. C. Barton and J. Hone, *Nano Lett.*, 2008, **8**, 982–987.
13 Z. Yang, T. Chen, R. He, G. Guan, H. Li, L. Qiu and H. Peng, *Adv. Mater.*, 2011, **23**, 5436–5439.
14 K. Jiang, J. Wang, Q. Li, L. Liu, C. Liu and S. Fan, *Adv. Mater.*, 2011, **23**, 1154–1161.
15 B. Oregan and M. Grätzel, *Nature*, 1991, **353**, 737–740.
16 M. K. Nazeeruddin, A. Kay, I. Rodicio, R. Humphrybaker, E. Muller, P. Liska, N. Vlachopoulos and M. Grätzel, *J. Am. Chem. Soc.*, 1993, **115**, 6382–6390.
17 F. Sauvage, D. Chen, P. Comte, F. Huang, L. Heiniger, Y. Cheng, R. A. Caruso and M. Grätzel, *ACS Nano*, 2010, **4**, 4420–4425.
18 F. Gao, Y. Wang, D. Shi, J. Zhang, M. Wang, X. Jing, R. Humphry-Baker, P. Wang, S. M. Zakeeruddin and M. Grätzel, *J. Am. Chem. Soc.*, 2008, **130**, 10720–10728.
19 M. Durr, A. Schmid, M. Obermaier, S. Rosselli, A. Yasuda and G. Nelles, *Nat. Mater.*, 2005, **4**, 607–611.
20 H. Lindstrom, A. Holmberg, E. Magnusson, S. E. Lindquist, L. Malmqvist and A. Hagfeldt, *Nano Lett.*, 2001, **1**, 97–100.
21 X. Fan, Z. Chu, F. Wang, C. Zhang, L. Chen, Y. Tang and D. Zou, *Adv. Mater.*, 2008, **20**, 592–595.
22 M. R. Lee, R. D. Eckert, K. Forberich, G. Dennler, C. J. Brabec and R. A. Gaudiana, *Science*, 2009, **324**, 232–235.
23 B. Weintraub, Y. Wei and Z. L. Wang, *Angew. Chem., Int. Ed.*, 2009, **48**, 8981–8985.
24 D. Zou, D. Wang, Z. Chu, Z. Lv and X. Fan, *Coord. Chem. Rev.*, 2010, **254**, 1169–1178.
25 J. Liu, M. A. G. Namboothiry and D. L. Carroll, *Appl. Phys. Lett.*, 2007, **90**, 133515.
26 D. Wang, S. Hou, H. Wu, C. Zhang, Z. Chu and D. J. Zou, *J. Mater. Chem.*, 2011, **21**, 6383–6388.
27 S. Hou, X. Cai, Y. Fu, Z. Lv, D. Wang, H. Wu, C. Zhang, Z. Chu and D. Zou, *J. Mater. Chem.*, 2011, **21**, 13776–13779.
28 X. Cai, S. Hou, H. Wu, Z. Lv, Y. Fu, D. Wang, C. Zhang, H. Kafafy, Z. Chu and D. Zou, *Phys. Chem. Chem. Phys.*, 2012, **14**, 10076–10083.
29 M. Zhang, K. R. Atkinson and R. H. Baughman, *Science*, 2004, **306**, 1358–1361.
30 Q. Li, Y. Li, X. Zhang, S. B. Chikkannanavar, Y. Zhao, A. M. Dangelewicz, L. Zheng, S. K. Doorn, Q. Jia, D. E. Peterson, P. N. Arendt and Y. Zhu, *Adv. Mater.*, 2007, **19**, 3358–3363.
31 H. Peng, X. Sun, F. Cai, X. Chen, Y. Zhu, G. Liao, D. Chen, Q. Li, Y. Lu, Y. Zhu and Q. Jia, *Nat. Nanotechnol.*, 2009, **4**, 738–741.
32 C. Perez Leon, L. Kador, B. Peng and M. Thelakkat, *J. Phys. Chem. B*, 2006, **110**, 8723–8730.
33 F. Liu, N. A. Hashim, Y. Liu, M. R. M. Abed and K. Li, *J. Membr. Sci.*, 2011, **375**, 1–27.
34 J. Y. Song, Y. Y. Wang and C. C. Wan, *J. Power Sources*, 1999, **77**, 183–197.
35 Z. Huang, X. Liu, K. Li, D. Li, Y. Luo, H. Li, W. Song, L. Chen and Q. Meng, *Electrochem. Commun.*, 2007, **9**, 596–598.

